DECLARATION

I, **Manash Protim Hazarika**, hereby declare that the thesis entitled **"Melting of Copper Metal with Imperfections: A Molecular Dynamics Simulation Study"** submitted by me for the award of **Master of Philosophy (M.Phil.) Degree in Chemistry** of Sikkim University is my original work. The content of the thesis is based on simulations study which I have performed myself. This thesis has not been submitted for any other degree to any other university. The content of this M.Phil. Dissertation has been subjected to the Anti-Plagiarism Software (Urkund) and it was found satisfactory
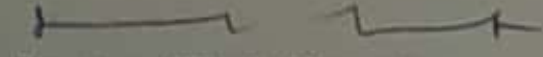
Date: 07.02.2019

Manash Protim Hazarika

Manash Protim Hazarika
Roll No. 17MPCH03

We recommend that the thesis be placed before the Examiners for evaluation.

Signature of Supervisor
Dr. Somendra Nath Chakraborty

Signature of Head of Department
Dr. Somendra Nath Chakraborty

सिक्किम विश्वविद्यालय
SIKKIM UNIVERSITY

(A central university established by an Act of Parliament of India in 2007 and accredited by NAAC in 2015)

Certificate

This is to certify that the thesis entitled " **Melting of Copper Metal with Imperfections : A Molecular Dynamics Simulation Study**" submitted to Sikkim University in partial fulfillment of the requirements for the degree of **Master of Philosophy (Science) in Chemistry** embodies the result of *bona fide* research work carried out by **Mr. Manash Protim Hazarika** under my guidance and supervision. No part of the thesis has been submitted for any other degree, diploma, associate-ship, fellowship.

All the assistance and help received during the course of the investigation have been duly acknowledge by him.

Place: Gangtok

Date: 07.09.2017

Dr. Somendra Nath Chakraborty

M.Phil. Supervisor

Department of Chemistry

School of Physical Science

Sikkim University

PLAGIARISM CHECK CERTIFICATE

This is to certify that plagiarism check has been carried out for the following M.Phil. Dissertation with the help of **Urkund** software and the result is within the permissible limit decided by the University.

"Melting of Copper Metal with Imperfections: A Molecular Dynamics Simulation Study"

Submitted by
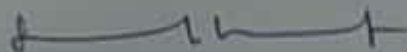
Manash Protim Hazarika

Under the supervision

of

Dr. Somendra Nath Chakraborty

Department of Chemistry

School of Physical Science

Signature of the Student

Countersigned by Head of Department

Melting of Copper Metal with Imperfections : A Molecular Dynamics Simulation Study

A Dissertation Submitted

To

Sikkim University

In Partial Fulfillment of the Requirement for the

Degree of Master of Philosophy

By

Manash Protim Hazarika

Department of Chemistry

School of Physical Science

February, 2019.

To my parents and brother...

Acknowledgements

Thank must go primarily to my supervisor Dr. Somendra Nath Chakraborty for his selfless advice, guidance and encouragement. It is a good experience working under the guidance and supervision of Dr. Somendra Nath Chakraborty. I would like to express my deep sense of gratitude and respect to him for giving me an opportunity to pursue my research interests in his group. I am grateful to him for his patience and willingness to discuss anything, be it about research or life in general which helped me to complete my work. Also I would like to thank him for his inspiration during the prepartion of my M.Phil dissertation work. Hopefully this thesis will contribute something to build upon for the future.

I am grateful to other faculty members, Dr. Biswajit Gopal Roy, Dr. Sudarsan Tamang, Dr. Anand Pariyar, Dr. Souvik Chatterjee for their support. They have always welcomed and motivated me from the very first day.

I would like to thank Mr. Mahabir Prasad and Mr. Sudarsan Karki, my lab seniors, for supporting and helping me during my work. I have learnt a lot about simulation softwares as well as fortan language from them. Also I want to thank my all friends, seniors in and out of Sikkim University for their love and support.

I would like to thank Sikkim University for financial suppot and for providig all aids needed during computational work.

Last, and definitely not the least, I pay special gratitude to my family members for their constant love, encouragement and support. My parents faith and sacrifices over the years have always kept me moving forward towards my goals.

Manash Protim Hazarika

Abstract

This thesis focus on computational studies of melting transition of copper crystal with volume voids. The melting properties of copper metal with different size of spherical voids, varied from 4 Å to 10 Å in radius and layered voids were studied by classical molecular dynamics simulations in isothermal-isobaric (NPT) ensemble. We used embedded atom method (EAM) potential for copper and obtain various thermodynamic and structural properties of copper crystals in the temeperature 900 K to 2000 K. Our objective was to find how spherical and layered voids influence the properties of solid and its bulk melting temperature. We calculated the potential energy, enthalpy, density, radial distribution function, order parameter (Q_6), diffusion coefficient and Lindemann index to characterize the melting process. Our results show that melting temperature is size dependent. Defects decrease the melting temperature from 1740 K to 1500 K. Melting temperature is also found to depend on the position of the defects.

Contents

List of Figures

List of Tables

Chapter 1

1 Bulk Melting

1.1 Preface

The process of solid becoming liquid with increase in temperature is called melting. During melting solid requires energy to transform to liquid and this energy goes exclusively to change the phase of the substance. Melting is thus classified as a first order phase transition where first derivative of Gibbs free energy with temperature and pressure changes discontinously. At the melting temperature, solid-liquid phase equilibrium exists and Gibbs free energy difference between phases are equal but entropy and volume of the two phases differ. Though many scientists proposed different theories for melting transition yet it's mechanism is not satisfactorily understood.
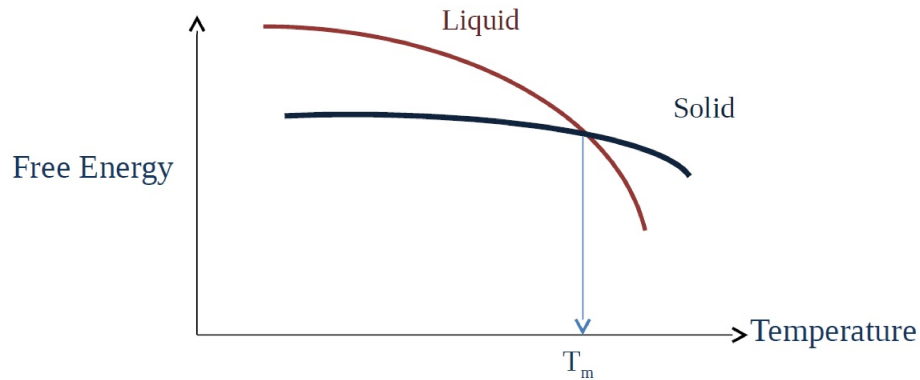
Figure 1.1: Variation of the Gibbs free energy of a simple atomic substance near the melting point as a function of temperature.

For all known elements (except He), the entropy of the liquid state is higher than that of the entropy of solid state at melting temperature.

$$\Delta S_m = Rl_n\left(\frac{W_l}{W_s}\right) \tag{1.1}$$

Where ΔS_m is the difference of entropy between the solid and liquid phases, R is the gas constant. W_l and W_s are the number of impartial methods of figuring out the molten state and solid state respectively. Melting is also a transition from an ordered state to a much less ordered state and thus melting increases the "randomnes" of the material [1]. Thermodynamic equations establish relationship between various macroscopic properties at melting. But mechanism of melting can't be explained properly by these equations. Mechanistically, melting transition is best understood by following structural changes taking place in materials during appearance of molten state.

One can find few theories suggested by researchers to describe the melting transition. According to Sorkin [2], all melting transitions can be divided into two groups. The first is the group of one phase models considering melting as a homogeneous (mechanical melting) process. It happens in the bulk of the solid resulting from lattice instability. The second group considers melting as a heterogeneous two-phase (thermodynamic melting) process resulting from extrinsic defects (grain boundary, voids etc.). Although homogenous melting theories are questionable yet these give a very simplistic perspective of this transition.

Two of the most important theories of melting which has been tested since they were proposed is discussed in the next two sections -

1.2 Lindemann Criterion

Frederick Lindemann [3] was the first scientist who explained the mechanism of melting. He proposed that melting happens when vibrational amplitude becomes half of the interatomic spacing in the crystal lattice [4]. When the temperature of solid is increased, vibrational amplitude of atoms also increase. At some point, melting occurs when the amplitude of vibrations become so large that atoms are completely displaced from their positions. Based on this Lindemann suggested an easy criterion that melting occurs when the root mean vibrational amplitude $\sqrt{\langle u^2 \rangle}$ exceeds a certain threshold value. Lindemann believed that each atom vi-

brates around their equilibrium position with the same frequency ν_E (the Einstein approximation). The average thermal vibration energy can be considered from the equipartition theorem as:

$$E = m4\pi^2\nu_E^2\langle u^2\rangle \tag{1.2}$$

Where m and ν_E are the atomic mass and Einstein frequency respectively. One can calculate the melting point using $\langle u^2\rangle = C_l^2$. C_l is the Lindemann constant.

There are few disadvantages of Lindemann theory. The theory is based on harmonic forces, while melting has to involve bond breaking. Moreover many experiments performed at excessive pressures suggest that the Lindemann model does no longer estimate accurately the strain dependence of the melting temperature [5]. The most serious drawback of the theory is that melting is defined in term individual atomic property, i.e. mean square amplitude of vibration, at the same time phase transition is a collective process [1]. Also, the Lindemann model consider melting for solid alone, even through the melting transition must involve in each solid and liquid phases.

1.3 Born Criterion

In the year 1939, Born [6] proposed a theory where he suggested that melting takes place when shear modulus becomes zero. He realized that liquid phase do not offer any resistance to shear stress unlike the crystal phase. A. Kanigel *et al.* [7] found that at melting point the Born hypothesis is fulfilled and showed that one of the shear stress of solid vanishes.

Shear elastic constant decrease with increasing temperature of solid substance because of the thermal development the distance between the atoms is decreased. Born investigated that the free energy of a solid with a cubic crystalline lattice. For a lattice to be stable, the free energy should be in quadratic form. For a

cubic crystal, there are three independent elastic constant: C_{11}, C_{12}, C_{44} and the accepted stability criteria are

$$C_{11} + 2C_{12} > 0 \tag{1.3}$$

$$C_{44} > 0 \tag{1.4}$$

$$C_{11} - C_{12} > 0 \tag{1.5}$$

Equation (1.3), (1.4) and (1.5) are related to bulk, shear and tetragonal shear moduli respectively and are referred to as spinodal, shear and Born criteria [8].

According to Born [6], C_{44} first vanishes and the melting temperature can be calculated from the relation $C_{44}(T_m) = 0$. He did not consider the external pressure. The new modified stability criteria are

$$C_{11} + 2C_{12} - P > 0 \tag{1.6}$$

$$C_{44} - P > 0 \tag{1.7}$$

$$C_{11} - C_{12} - P > 0 \tag{1.8}$$

Experimentally melting can be located in various ways. A simple technique is to note the temperature at which molten state of the solid state first appears. Other sophisiticated techniques to locate melting are calorimetric measurements etc. These methods help to locate the melting temperature of the sample precisely. But experimentally, it is always hard to understand melting inside a crystal since this process takes place during a short interval of time. To understand these aspects of melting theoretical and computational studies are performed. Molecular simulations have played an important role in understanding melting transitions in bulk. One of the most important conclusions obtained from simulatios is that mechanical melting occurs after thermodynamic melting. Wang *et al.* [9] analyzed the bulk melting temperature of copper without external pressure using molecular

dynamics simulation and found that shear moduli $C^/$ vanishes at some temperature, T_f, which is higher than thermodynamic melting that is $T_f > T_m$. They also concluded that Born stability criteria is satisfied only for perfect crystal; not for real crystals with defects and boundaries.

According to Frenkel [10], melting happens because of formation and spreading of intrinsic crystalline defects like vacancies. Lennard-Jones and Devonshire [11, 12] proposed a theory which depended on positional disordering. They considered a model of rare gas crystal and first order transition was observed. Their theory was based on order-disorder transition. The disadvantage of this theory was that it proposed a critical point for melting which was not observed experimentally. Out of all the theories for melting, Lindermann and Born theories are mostly used to examine the melting transition.

Moreover simulation studies also show that spread of defects cause melting. It has also helped to understand the effect of imperfections like point defects, voids, grain boundaries, dislocations etc. in crystals. These aspects which are otherwise impossible to study experimentally has been successfully investigated from molecular simulations. [13]

As explained previously both Monte Carlo and Molecular Dynamics simulations have been extensively used to study melting. Advanced sampling technqiues have also been used to estimate free energies of solid and liquid basins at the melting temperature. Most of the earlier simulations on melting were performed on Lennard-Jones potential. Later melting of ice and metallic systems have been investigated with more reliable potentials which could reproduce experimental properties of these systems reasonably well. Both Lindemann and Born criteria of melting have been rigorously tested for these systems.

Melting of metallic systems and its alloys has remained an active area of research since a long time. One of the most studied metallic system is copper. It is one of those materials we use throughout the day in a variety of forms due to remarakable physical properties. Its a good conductor of electricity and its ductility

makes it the most suitable metal avaialble for conduction. At ambient conditions copper has a melting temperature of 1356 K. The melting properties of copper in bulk, clusters and with defects are being researched exhaustively using simulation methods.

Point defects and voids play an important role in melting. The physical properties of the solid depend on point defects and nano-voids. Interstitials extend the sample, while vacancies diminish its volume. A.Kanigel *et al.* [7] discovered that the bulk melting temperature of copper depends on the concentration of point defects (namely self-interstitials). Point defects expand the volume of the solid to a critical value at which the mechanical melting transition is produced. According to A.Kanigel *et al.* [7] the bulk melting transition is lowered by point defects.

Recently melting of copper metal with imperfections and also under shock have generated lots of interest. With the availability of reliable potentials for copper, both MC and MD techniques have been widely used to study this system. Our focus in this thesis is to understand mechanism of melting in copper with imperfections. We analyse the structural properties of copper around the melting transition. We create two types of imperfections in bulk copper and investigate structural changes asociated with melting.

In the next chapter we briefly review the literature available on melting of bulk metal like copper, aluminium etc. with defects and melting of copper clusters. We review the simulation studies performed on these systems.

Chapter 2

2   Review of Literature

This chapter briefly reviews the literature on simulation studies of melting with defects and melting of nano-clusters. In the first section literature on melting studies of copper, aluminium, Lennard-Jones systems with defects is reviewed. Second section presents the review on melting of copper and LJ nano-clusters.

2.1   Melting of Defective Bulk Metal

In a recent work melting pathways have been determined using advanced sampling techniques in molecular dynamics simulations. According to Samanta *et al.* [14] melting of solid happens through multiple melting pathways and each pathway proceeds via the formation of point defects and dislocations. Melting is aided through mobile defect each at the thermodynamic melting point and at super-heating. They established three specific melting regimes in their rare sampling simulation of copper:

(i) Close to melting transition occurs via multiple barrier crossings.

(ii) At superheated temperature (1525 K to 1595 K), melting occurrs as single barrier crossing event and it consists of both entropic and enthalpic contribution.

(iii) Beyond the superheating, melting is driven by large vibrational amplitudes of atoms.

To determine the structural and thermodynamics melting point of copper, Lutsko *et al.* [15] simulated bulk copper with a grain boundary and voids on (001) plane using EAM potential at superheating rate and found the structural and thermodynamic melting at 1450 K and 1171 K individually. They found that the ratio between structural and thermodynamic melting points is 1.32.

Puri *et al.* [13] performed molecular dynamics simulation using isobaric-isoenthalpic ensemble to investigate the effect of voids on the melting of bulk Aluminum within

7

the size range varied from 2 nm 9 nm. To characterize the melting process, they analyzed Lindemann index, translational order parameter and radial distribution function and found that melting temperature is dependent on the size of voids. Voids decrease the melting point and the structural melting point of bulk Al with void was also found to be 32% higher than the thermodynamic melting point.

In the year 1998, P.Heino *et al*. [16] studied the mechanical properties of copper with various types of defects from molecular dynamics simulation using effective medium theory (EMT) [17]. They investigated the physical properties of three types of defects: point defects, grain boundary, and an initial void serving as a crack seed. Simulations were done at room temperature or near zero temperature. First they studied the strength and modulus of copper with vacancies or interstitials where they removed atoms randomly from the perfect fcc structure to introduce vacancies and added atoms randomly to the perfect fcc structure such that two atoms were not too close to each other to introduce the interstitials. They found that system strength was decreasing in terms of fracture stress and fracture strain as they increased the amount of defects and the inerstitials decreased the system strength more effectively than vacancies. They studied the effect of grain boundaries with different crystal orientations introducing one such boundary and found that elastic modulus and the critical strain for crack initiation turned into less on the grain boundary than in the bulk of the system.

In 2008, Li-Boo Han *et al*. [18] investigated the isobaric melting of defective copper solids by classical molecular dynamics simulations using EAM interatomic potential [19]. They introduce only one type of defect: intrinsic or extrinsic stacking faults. Simulations were performed under steady pressure-temperature ensemble and three dimensional periodic boundary condition was applied. Hoover thermostat [20] and isotropic volume scaling [21] was applied to control the Temperature and pressure respectively. They found that global order parameter for both intrinsic and extrinsic stacking faults was diminished from 0.94 at 300 K to 0.44 at 1600 K and dropped quickly to 0.115 at 1620 K (melting point). From the

development of enthalpy and density at 1620 K, they mentioned that the melting point of both the defective copper and perfect copper was 1620 K which implies that the stacking faults have little or insignificant impacts on the bulk melting at such high heating rates. The authors mentioned that nucleation of liquid nuclei happened close to the stacking fault indicating both heterogeneous and homogeneous nucleation and the stacking faults slightly expanded the nucleation rate.

2.2 Melting of Nanostructures

In the year 2003, Li Wang and his co workers [22], studied the melting behavior of copper nanocluster within up to 8628 atoms by molecular dynamics simulation using embedded atom method (EAM) [19]. The calculation was performed in two steps. First, they simulated the nanoclusters with constant temperature and constant volume (NVT) without the periodic boundary condition. After that, the bulk system was simulated under constant temperature and constant pressure (NPT) condition containing up to 500 particles in the cube with a periodic boundary condition. They defined the melting point as the temperature corresponding to the maximum of the heat capacity. In their work, heat capacity indicates the melting point is 1780 K. They also found that there exists an intermediate region above 456 atoms, the melting temperature and heat of melting scales inversely as $N^{-1/3}$ for FCC structures in this region. Melting of the whole clusters begin from the liquid to core region and the enthalpy, entropy and the surface energy of the clusters increase with the increase of cluster size.

H.H.Kart *et al.* [23] studied the thermodynamics, structural and dynamics properties of copper nanoparticles containing from 369 atoms to 44,403 atoms, diameter varied from 2 nm to 10 nm by molecular dynamics simulation using Quantum Sutton-Chen (QSC) [24] many-body force potential. All the calculations were done in the MPiSiM software developed at Caltech [25] under NVT condition. They investigated that how the melting temperature, heat capacity, radial distribution function, mean square displacement, diffusion coefficient, Lindemann

9

index and Honeycutte Andersen index of nanoparticles are depend on nanoparticle sizes, including pre-melting of the nanoparticles to estimate the phase transition from solid to liquid. In their work, they found that melting temperature of Cu nanoparticles increased as they increased the size of the nanoparticles and from the Honeycutte Andersen index plot they found that the number of fcc atoms were decreased with increasing the temperature. They also calculated the diffusion co-efficient using the slope of MSD curve and found to be fitted with the Arrhenius curve. From the Lindermann index plot, they concluded that an increase in temperature leads to an increment of the surface diffusion or surface melting of the nanoparticles.

In 2017, Jiacheng Zhang *et al.* [26] studied the melting behaviors of copper nanorod by using molecular dynamics simulation using embedded atom method potential. Calculations have been calculated using large-scale atomic/molecular massively parallel simulator (LAMMPS) [27] under NVT condition with an integration time step of one femtosecond to simulate the melting conduct of the copper nanorods. The periodic boundary condition became implemented to all the three axial direction. They presented the copper nanorods with five unique diameters of 2.896, 3.62, 4.344, 5.43, 6.516 nm including 4036, 8081, 13446, 26942, 45905 atoms respectively. They identified the melting point of copper nanorods by the slop fast change in the potential energy curve. According to them, melting temperature is strongly size-dependent and the nanorod with smaller diameter has a decrease melting temperature. It was seen that in case of surface atoms, potential energy was higher than the interior ones. The proportion of the surface atoms is bigger for the nanorod with a smaller diameter, which decrease the melting point. They observed that that copper nanorods go through two thermal structural modifications throughout the heating process: shape transition and melting transition. The shape transition followed the incidence of planar defects like twin boundaries and stacking faults. After accomplishing melting point, the intermediate structure collapsed into a liquid sphere.

As observed earlier by Solca [28] and later by Aggarwal [29], melting temperature decreases with size of the voids. Thereafter a plateau region is observed wherein the melting temperature does not change with the size of the void. It was also reported by Agarwal that melting temperature does not depend on the shape of the void. Moreover in another study by Bai and Li [30] showed that melting in void systems occur in four stages. They simulated lenard jones system having voids of size 0.58 to 6.62 nm. They found that voids collapse and acts as seeds for melting of the crystals. We test these observations in our study. Our study aims at the following - first we investigate melting in systems with smaller voids ranging from 4 to 10 Å. Second we change the shape and position of the void and analyse its effect on the melting properties.

Chapter 3

3 Computational Details

3.1 Idea of Molecular Dynamics

In our work, we have performed Molecular Dynamics (MD) simulations to analyze the properties of copper and copper with spherical and layered voids. Molecular dynamics simulation is a statisitical tool for computer based simulation of atoms and molecules [31]. In this method, molecules are allowed to have interaction with every different atom in the system for a certain time frame. For a system of interacting particles, the paths are decided by solving the Newton's equations of motion, where forces among particles are calculated using force fields. The goal of the MD simulation is to predict the time-based trajectories in a system of interacting particles [32].

In our work we use Verlet [33] algorithm to integrate the Newtonian equation of motion with an integration time-step of 2 fs. Two interatomic potentials, embedded atom method (EAM) and charge optimize many body potential (COMB) for Copper proposed by Folis [19] and Liang [34] respectively are chosen for our calculations. Simulations are carried out using large-scale atomic/molecular massively parallel simulator (LAMMPS) [27] in NPT ensemble. Cubic periodic boundary conditions are applied in all the three axial directions.

A Molecular Dynamics algorithm is explained here - (i) Firstly, the initial positions from X-ray diffraction data and velocities from Maxwell-Boltzmann distribution of each atom are described.

(ii) The forces between the atoms are calculated through the usage of the inter-atomic potentials.

(iii) As soon as we get the forces, a small time interval is introduced, and the initial atomic positions and velocities change to a new values.

(iv) The process is repeated till the end of the simulation.
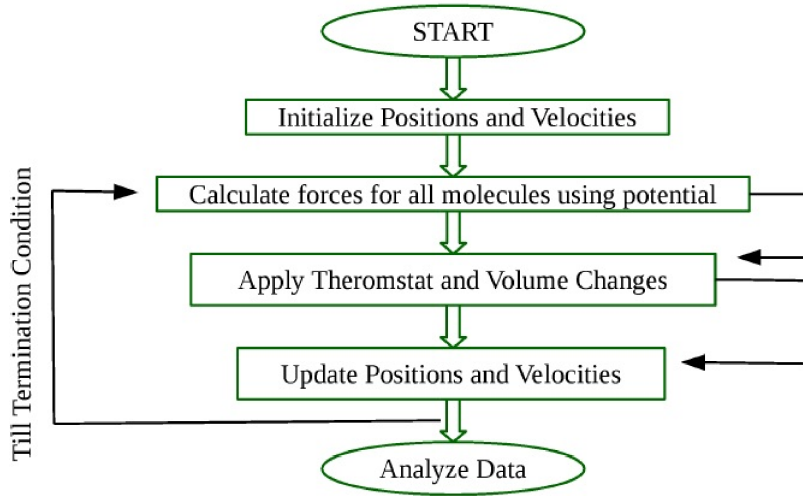
Figure 3.1: A simple molecular dynamics program.

3.2 Interatomic Potential

To start MD simulation, we need model and these models are often expressed in terms of potential function. The potential function defines how the potential energy of a system of N atoms depend on the coordinates of the atoms. In classical MD simulation, electrons are not taken into account and Newtonian equation of motion is solved.

The total energy of the N atoms system with empirical potential is written as

$$U(\vec{r_1}, \vec{r_2}, ...\vec{r_n}) = \sum_i U_1(r_i) + \sum_i \sum_{j>i} U_2(\vec{r_i}, \vec{r_j}) + \sum_i \sum_{j>i} \sum_{k>j} U_3(\vec{r_i}, \vec{r_j}, \vec{r_k}) + ... \quad (3.1)$$

Where U_1 stands for one body term due to an external field or boundary condition. The second term, U_2 indicates pair wise potential and the third term, U_3 gives the three body component when the interaction of pair of atoms is changed by the presence of a third atom.

While selecting potentials one has to consider the following properties:

(i) Accuracy (reproduce qualities of interest as closely as possible)

(ii) Computational speed (calculations are rapid with simple potentials)

In molecular dynamics simulation it is hard to consider the interactions between one atom and the other atoms present in the simulated system. To decrease the computational effort only the closest neighbors of every atom are taken account. Therefore, a cut-off radius is introduced as a highest value of the modulus of the radius vector [32]. Because of this, the interactions among the atoms are taken within the cut-off radius.

3.2.1 Embedded Atom Method

Embedded atom method was first proposed by Dow and Baskes in 1987 [35] and it has been mostly used for the simulation of matter at the atomic level. EAM is based on density functional theory (DFT) [36].

In the embedded atom method, each atom is embedded in a host electron gas generated by all surrounding atoms [32]. The amount of energy needed to put one atom into the electron gas of a given density is called the embedding function, which considers many atom effects. In a simulation, the potential energy of an atom, i, is given by-

$$E_i = F_\alpha \left(\sum_{i \neq j} \rho_\beta(r_{ij}) + \frac{1}{2} \sum_{i \neq j} \phi_{\alpha\beta}(r_{ij}) \right) \tag{3.2}$$
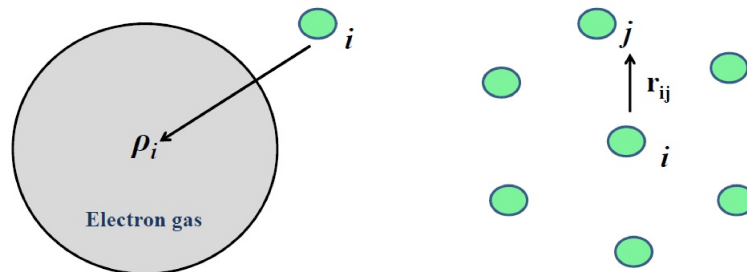
where r_{ij} is the distance between atoms i and j , $\phi_{\alpha\beta}$ is a pair-wise potential function, ρ_β is the contribution to the electron charge density from atom j of type

β at the location of atom i, and F is an embedding function that represents the energy needed to put atom i of type α into the electron cloud [32].

3.2.2 Charge optimized many-body potential(COMB)

We have also used COMB potential for the simulation of small number of Cu atoms (n=500). The COMB potential is a variable charge potential. The equilibrium charge on each atom is calculated by the electro negativity equalization [37]. In a simulation, the energy 'E' of system of atoms is given by

$$E_T = \sum_i \left[E_i^S + \frac{1}{2} \sum_{j \neq i} V_{ij}(r_{ij}, q_i, q_j) + E_i^{BB} \right] \tag{3.3}$$

$$V_{ij}(r_{ij}, q_i, q_j) = U_{ij}^R(r_{ij}) + U_{ij}^A(r_{ij}, q_i, q_j) + U_{ij}^I(r_{ij}, q_i, q_j) + U_{ij}^V(r_{ij}) \tag{3.4}$$

Where E_T is the total potential energy of the system, E_i^S is the self-energy of atom i. V_{ij} is the interatomic potential between the ith and j^{th} atoms, r_{ij} is the distance between the atoms i and j, and q_i and q_j are charges of the atoms, and E_i^{BB} stands for bond-bending term of atom i.

The interatomic potential energy V_{ij} has four parts. U_{ij}^R, U_{ij}^A, U_{ij}^I and U_{ij}^V stand for two-body short-range repulsion, many-body short-range attraction, long-range Coulombic electrostatic interaction, and van der Waals energy respectively [37].

3.2.3 Melting of Bulk Copper Using COMB and EAM Potential

Before introducing the defects, we simulated a small crystal system of copper containing 500 atoms using EAM and COMB potentials.
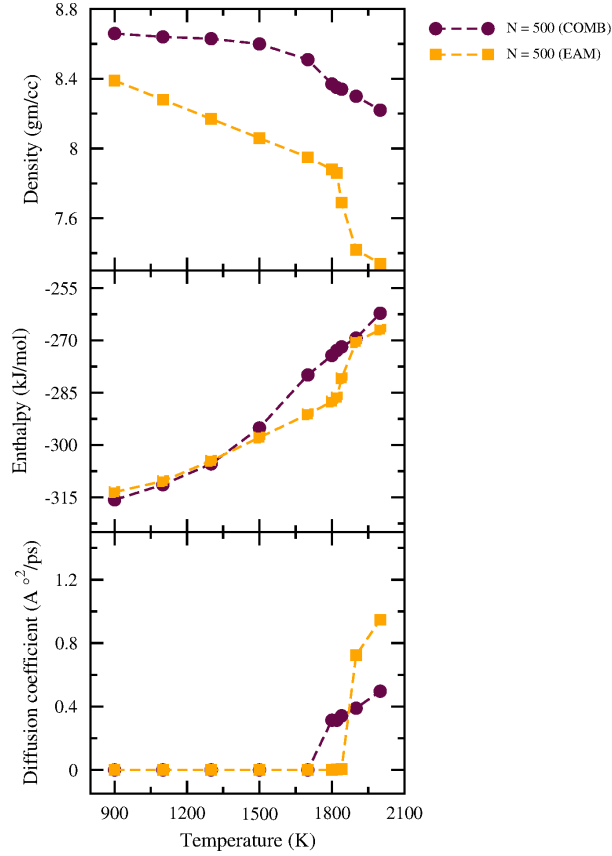
Figure 3.2: Density, enthalpy and diffusion coefficient as a function of temperature of bulk copper (500 atoms).

From the figure 3.2, it is seen that densities obtained from both the potential are different while enthalpy and diffusion coefficient agree for both COMB and EAM potential. At ambient pressure, elting point is found to be 1780 K from EAM potential which is closer to the available theoretical data [22]. Also we have found that COMB potential is very time consuming and EAM calculations are five times faster than COMB. Therefore, we choose EAM potential for all our simulations.

3.3 Newtons equation of motion

The dynamics of classical objects follow the three laws of Newton. We get the equation of motion for classical particles from Newton's second law. Consider, the position of a particle is described by a vector $r = (x,y,z)$. The velocity changes with time and is also a vector: $v = dr/dt = (v_x, v_y, v_z)$. In component form, $v_x = dx/dt$, $_y = dy/dt$, $v_z = dz/dt$. The acceleration vector is then time derivative of velocity, i.e., $a = dv/dt$ [38]. So that, equation of motion for particle can be written as-

$$\frac{d^2 r}{dt^2} = \frac{F}{m} \tag{3.5}$$

Where force is calculated from

$$F = -\frac{dV(r)}{dr} \tag{3.6}$$

Now we have the complete equation of motion for particle

$$\frac{d^2 r}{dt^2} = -\frac{1}{m}\frac{dV(r)}{dr} \tag{3.7}$$

Where $V(r)$ is the potential energy of the system and the kinetic is given by-

$$E_{kin} = \frac{1}{2}m|V|^2 \tag{3.8}$$

The total energy is the sum of kinetic and potential energy contribution.

$$E_{tot} = E_{kin} + V \tag{3.9}$$

Since we consider the total energy as a function of particle position r and momentum $p = mv$, it is called the *Hamiltonian* of the system,

$$H(r,p) = \frac{|p|^2}{2m} + V(r) \tag{3.10}$$

The Hamiltonian (i.e. the total energy) is preserved if the particle obeys the Newtons equation of motion.

$$\frac{dE_{tot}}{dt} = mv\frac{dv}{dt} + \frac{dV(r)}{dr}\frac{dr}{dt} = m\frac{dr}{dt}\left[-\frac{1}{m}\frac{dV(r)}{dr}\right] + \frac{dV(r)}{dr}\frac{dr}{dt} = 0 \tag{3.11}$$

Therefore, the total energy is a conserved quantity when the particle moves. We can also write the Newtons equation of motion in the form of Hamiltonian.

$$\frac{dr}{dt} = \frac{\partial H(r,p)}{\partial p} \tag{3.12}$$

$$\frac{dp}{dt} = \frac{\partial H(r,p)}{\partial r} \tag{3.13}$$

$$\frac{dH}{dt} = \frac{\partial H(r,p)}{\partial r}\frac{dr}{dt} + \frac{\partial H(r,p)}{\partial p}\frac{dp}{dt} = 0 \tag{3.14}$$

3.4   Time Inegration Algorithm

A dynamical simulation calculates the new position of particle as a function of time from its initial position and velocity [38]. Since the 'r' in Newtonian equation of motion is second order, therefore, the initial condition needs to define both particle position and velocity. To solve the Newtonian equation of motion, time is discretized using a time step Δt. The integration procedure gives the positions and some of their derivatives at a certain time $t + \Delta t$ [32]. Once those quantities are known on the previous time t, the time development of the system can be followed by iterating this procedure.

There are different kinds of time integration algorithms to solve the equation of motion. Each algorithm has its own advantages and disadvantages. Before choosing an algorithm, we should consider about the order of accuracy and reversibility of the integration algorithms [39].

3.4.1 Verlet Algorithm

In our simulation work, we have used Verlet algorithm [33] because it is simple to implement and time accurate In this algorithm two third order Taylor expansions for positions $r(t)$, one forward and the other backward in time is written [40].

$$r(t - \Delta t) = r(t) - v(t)\Delta t + \frac{1}{2}a(t)\Delta t^2 - \frac{1}{6}b(t)\Delta t^3 + O(\Delta t^4) \qquad (3.15)$$

$$r(t + \Delta t) = r(t) + v(t)\Delta t + \frac{1}{2}a(t)\Delta t^2 + \frac{1}{6}b(t)\Delta t^3 + O(\Delta t^4) \qquad (3.16)$$

Adding both equation, we get the basic form of the Verlet algorithm.

Since we are integrating Newtons equation, $a(t)$ is just the force divided by mass and force is in turn a function of this position $r(t)$.

$$a(t) = -\frac{1}{m}\nabla V(r(t)) \qquad (3.17)$$

But Verlet algorithm does not calculate velocities which is obtained from the positions using the following expression.

$$v(t) = \frac{r(t + \Delta t) - r(t - \Delta t)}{2\Delta t} \qquad (3.18)$$

3.4.2 Time Step

The choice of time-step Δt is an important factor in MD simulation. The time-step has to be small enough in order that the simulation is realistic and the integration

algorithm conserves the total energy of the system. If we choose a large time step, the motion of atoms is not continuous and the particles jump too far from their positions in each iteration which is also reflected in the potential energy as well as the total energy [41].

3.5   Periodic Boundary Condition

Proper boundary conditions are key to a successful atomistic simulation. In molecular simulation, we simulate a finite and comparatively small number of particles. This introduces surface effects. For example, in a simulation of cubic crystal consisting of 1000 particles, 521 will be at the surface [41]. But we need to compute the bulk properties of the system that means properties in the thermodynamic limit, $N \to \infty$. To get rid of the problem, periodic boundary conditions (PBC) are usually imposed. Here we use cubic periodic boudary conditions for all our simulations.
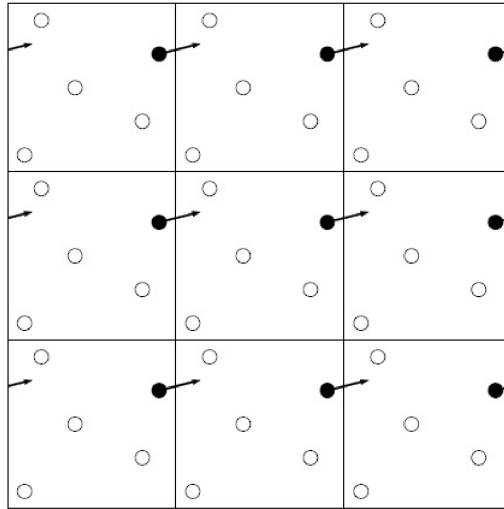

Figure 3.3: Periodic boundary conditions used in MD simulations, from ref [41]

When PBC is implemented, the simulation cell becomes an infinite, periodic array of replicas or images occupied by particles. The atoms within the replicas behave exactly in an identical manner as the atoms inside the main simulation cell. [39].

3.6 Isothermal-isobaric (NPT) ensemble

In classical molecular dynamics simulation, the isothermal-isobaric (NPT) ensemble is mostly used because; the real experiments are always performed under constant temeprature and pressure conditions. In experiments constant temperature and pressure is maintained typically using a heat bath. In this ensemble, the paritions function can be written as -

$$Q_{NPT} = \frac{1}{N!} \frac{1}{h^{3N}} \frac{1}{V_0} \int \int exp(-\beta(\mathcal{H}(r,p) + PV))drdpdV \qquad (3.19)$$

Where $\beta = 1/k_B T$ is the statistical temperature and V_0 is a reference volume. In this ensemble, sampling is done solving the equations of motion at a fixed temperature and pressure.

3.6.1 Molecular Dynamics at Constant Temperature

To implement the constant temperature condition we have to perform the sampling incontact with a heat bath. The energy here is Boltzmann distributed and the imposed macroscopic temperature is proportional to the average kinetic energy per particle [42].

$$k_B T = m \left\langle v_\alpha^2 \right\rangle \qquad (3.20)$$

Where v_α is the velocity of α th component amd m is the mass of the particle. In order to sample the instantaneous kinetic temperature T_k fluctuates around its macroscopic.

$$\frac{\sigma_{T_k}^2}{\left\langle T_k \right\rangle_{NVT}^2} = \frac{2}{3N} \qquad (3.21)$$

To control the fluctuation of the temperature, an algorithm called thermostat is used. In our work, we employed Nosé-Hoover thermostat, introduced by Nose

[43] and subsequently developed by Hoover [20]. Nosé-Hoover thermostat uses an extended Lagrangian containing additional coordinates and velocities [42]. Heat bath is thus introduced using additional coordinate s, associated with effective mass Q.

The resulting Hamiltonian of N particles with additional coordinate is

$$\mathcal{H} = \sum_{i=1}^{N} \frac{\mathbf{p}_i}{2m_i s^2} + U(\mathbf{r}^N) + \frac{p_\xi^2}{2Q} + L\frac{lns}{\beta} \tag{3.22}$$

Where ξ is the friction parameter and p_ξ is the momentum of the reservoir.

The following equations are used to calculate the difference between instantaneous kinetic temperature and the reference temperature.

$$\frac{d^2\mathbf{r}_i}{dt^2} = \frac{\mathbf{F}_i}{m_i} - \frac{p_\xi}{Q}\frac{d\mathbf{r}_i}{dt} \tag{3.23}$$

$$\frac{dp_\xi}{dt} = (T - T_0) \tag{3.24}$$

3.6.2 Molecular Dynamics at Constant Pressure

We have employed Nosé-Hoover barostat to control the pressure fluctuation during simulation. At constant pressure, the volume is interpreted as variable. Nosé-Hoover barostat was described by Martyna *et al.* [44] which is based on constant temperature method proposed by Anderson [45]. The equation of motion proposed by Martyna *et al.* are

$$\dot{\mathbf{r}}_i = \frac{\mathbf{p}_i}{m_i} + \frac{p_\epsilon}{W}\mathbf{r}_i \tag{3.25}$$

$$\dot{\mathbf{p}}_i = \mathbf{F}_i - \left(1 + \frac{d}{N_f}\right)\frac{p_\epsilon}{W}\mathbf{p}_i - \frac{p_{\xi_1}}{Q_1}\mathbf{p}_i \tag{3.26}$$

$$\dot{V} = \frac{dV p_\epsilon}{W} \tag{3.27}$$

$$\dot{p}_\epsilon = dV(P_{int} - P_{ext}) + \frac{d}{N_f} \sum_{i=1}^{N} \frac{\mathbf{p}_i^2}{m_i} - \frac{p_{\xi_1}}{Q_1} p_\epsilon \tag{3.28}$$

$$\dot{\xi} = \frac{p_\xi}{Q} \tag{3.29}$$

$$\dot{p}_\xi = \sum_{i=1}^{N} \frac{\mathbf{p}_i^2}{m_i} + \frac{p_\epsilon^2}{W} - (N_f + 1)kT \tag{3.30}$$

Where r_i and p_i are position and momentum of the i th particle respectively. V is the volume. p_ϵ, ξ and p_ξ are the barostat momentum, thermostat position and momentum respectively. P_{ext} is the external pressure and P_{int} is the internal pressure.

$$P_{int} = \frac{1}{dV} \left[\sum_{i=1}^{N} \left(\frac{\mathbf{p}_i^2}{m_i} + \mathbf{r}_i \mathbf{F}_i \right) - dV \frac{\partial U(V)}{\partial V} \right] \tag{3.31}$$

Where U is the potential.

3.7 Visualization and Initial Configurations

For MD simulation, visualization is so essential for the development of the work. The complicated geometry of copper crystal and spherical void configurations inside the bulk and the correct implementation of periodic boundary conditions are tested by "Visual Molecular Dynamics" (VMD) [46] visualization tool. VMD was used extensively in our research work. It is a very powerful visualization tool which helps to improve the 3D observation.
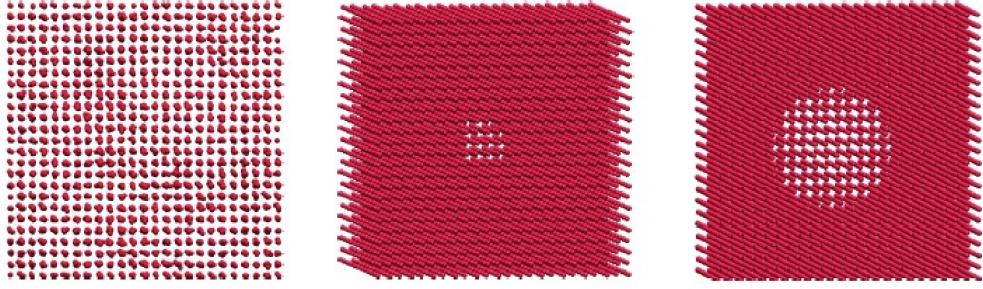
Figure 3.4: Initial structure of 12x12x12 supercell of copper without void and with small and large radius of spherical void.

- Five different model systems of bulk Cu with different size of spherical void having radius 4-10 Å were generated.

- All models were equilibrated over 2500000 time steps at elevated temperatures ranging from 900 K to 2000 K at an interval of 100 K after that the equilibrated configurations were simulated for production run over 500000 time steps.

The model system of bulk fcc copper without spherical void containing 6912 atoms.

Radius of spherical void	Number of atoms
4Å	6886
5Å	6874
6Å	6832
8Å	6730
9Å	6667
10Å	6542

Table 3.1: Number of copper atoms present in different system of voids having radius 4-10 Å

We have also analysed melting properties of bulk copper with other defects like layered voids. We removed 370 atoms from the center and edge of the bulk copper containing 6912 atoms.
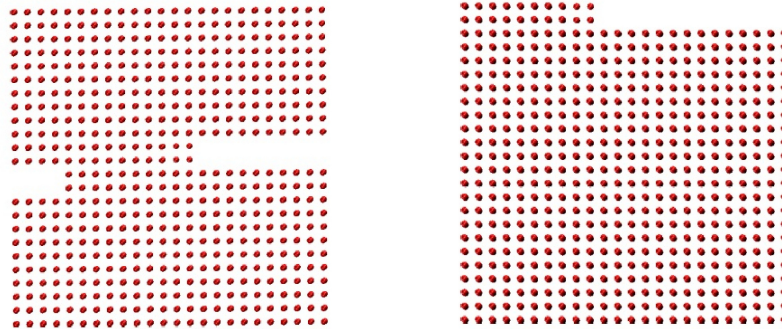
Figure 3.5: Initial structure of 12x12x12 supercell of copper with layered voids.

3.8 Simulation using LAMMPS

Large-scale atomic/molecular massively parallel simulator (LAMMPS) [27] software was chosen to perform this simulation. LAMMPS is molecular dynamics simulation, open source code written in C++ language [37].

This software can model a set of particles in a solid, liquid or gaseous state and additionally atomic, metal and biological systems the usage of various types

of boundary conditions and force fields. LAMMPS integrates Newton's equations of motion for group of molecules, atoms, or macroscopic particles which interact by short- or long-range forces [37].

There are two essential things that LAMMPS needs to run a Molecular Dynamic simulation, which are the input script and a potential file. The first one is where all the instructions that the program will need are written. The potential file is the one that includes the parameters of the interatomical potential of the simulated system.

A LAMMPS input script has 5 parts:

1. Initialization

2. Atom and Lattice definition

3. Force fields

4. Settings

5. Run

In the LAMMPS software, the"metal" units are: distance = Å, time = picoseconds, energy = eV, velocity = Å/ps, temperature = K, pressure = bar [37]

An example of input file using in our simulation for fcc copper containing 6912 atoms.

Initialization

units   metal

(specifies units of every quantity used in the input file)

dimension   3

(simulation dimensions, in this case 3D)

boundary   p p p

(for x, y and z direction, the boundary is periodic)

Atom and Lattice definition

region box   block 0 12 0 12 0 12 units box

(defines a geometric region of space)

create box   1 box

(generates a simulation cell in the defined region)

lattice   fcc 3.615

(lattice type and lattice parameter)

region   Cu block 0 12 0 12 0 12 units box

create atoms   1 region Cu units box

(generates copper atoms in the simulation)

Force fields

pair style   eam/alloy

*pair coeff   * * Cu.eam.alloy*

("*" indicates that the potential is applied to all the types of atoms defined.)

Settings

velocity all create   900 12345

(sets the velocity of a group of atoms)

fix 1   all npt temp 900 900 0.01 iso 1 1 1000 drag 1

(temp and pressure conserved)

thermo   100

(computes and prints thermodynamic data every 100 timesteps)

thermo style   custom step temp etotal pe ke enthalpy lx ly lz press density

(specifies content of thermodynamic data to be printed in screen)

Run the simulation

timestep   0.002

(sets the timestep for subsequent simulations)

run   500000

(program is run for 500000 iterations)

SIMULATION DONE

print "All done"

3.9   Quantities of Interest

In our simulation work, we have analyzed structural and thermodynamic properties like density, enthalpy, radial distribution function (RDF), diffusion coefficient and order parameter (Q_6) to characterize the melting process.

- **Density**

$$\langle \rho \rangle = \frac{mN}{\langle V \rangle} \tag{3.32}$$

- **Enthalpy**

$$\langle H \rangle = E + P \langle V \rangle \tag{3.33}$$

- **Diffusion Coefficient** (D)

Diffusion coefficient can be calculated from the slop of mean square displacement (MSD) at long time gap [23]. MSD helps us to examine the motion of the atoms of the model system before and after the melting point. It is a quantity of average distance that a given particle in system travels. The MSD define as [47]

$$MSD = \langle r^2(t) \rangle = \left\langle \frac{1}{N} \sum_{i=0}^{N} (r_i(t) - r_i(0))^2 \right\rangle \tag{3.34}$$

where N and t stands for number of particles and time respectively. $r_i(t) - r_i(0)$ is the vector distance traveled by a given particle over time interval.

The Einstein formula is used to calculate diffusion coefficient [48].

$$D = \frac{1}{6} \lim_{t \to \infty} \frac{d}{dt}(MSD) \tag{3.35}$$

• Lindemann index

The melting transition temperature is often defined by root mean square bond fluctuation, called Lindemann index δ [23]. The Lindemann index of each atom and of the entire bulk system is calculated by following formulas [49].

$$\delta_i = \frac{1}{N-1} \sum_{j \neq i} \frac{\sqrt{\left\langle r_{ij}^2 \right\rangle_T - \left\langle r_{ij} \right\rangle_T^2}}{\left\langle r_{ij} \right\rangle_T} \tag{3.36}$$

$$\delta = \sum_i \delta_i \tag{3.37}$$

Where N is the number of atoms. δ_i and δ are the Lindemann indices of i th atom and bulk respectively, r_{ij} is the distance between i th atom and j th atom.

• Radial distribution function (RDF)

RDF is used to analyze the structural properties of materials. RDF of single type of atom in a system defined as [23]

$$g(r) = \frac{V}{N} \frac{n(n)}{4 \Pi r^2 \Delta r} \tag{3.38}$$

Where V and N are the volume and number of particles in the system respectively, and $n(r)$ is the number of atoms in the thickness of Δr at the radius of the particle.

• Bond order parameter (Q_6)

Bond order parameters are introduced by Steinhardt [50]. Bond order parameters are based on spherical harmonics [51]. From the value of bond order

parameter, one can determine the crystal structure in molecular simulation. For each atom, bond orientation order parameter is calcultaed by following equations [52].

$$\bar{Y}_{lm} = \frac{1}{nnn} \sum_{j=i}^{nnn} Y_{lm}\Big(\theta(r_{ij}), \phi(r_{ij})\Big) \tag{3.39}$$

$$Q_l = \sqrt{\frac{4\Pi}{2l+1} \sum_{m=-l}^{m=l} \bar{Y}_{lm}\bar{Y}_{lm}^*} \tag{3.40}$$

First equation indicates the spherical harmonic order parameter. The summation over the nnn stands for nearest neighbor of the central atom. θ and ϕ are the standard spherical polar angles. Q_l in the second equation is rotationally invarient scaler quantity [52].

Chapter 4

4 Results and Discussions

We perform molecular dynamics simulations of copper with two types of volume defects. In the first case spherical voids of different sizes are introduced in the crystal. In the second rectangular shaped layers are removed from two places of the crystal and then melting transition is ivestigated in them. All simulations were performed at 1 bar and temperatures were varied from 900 to 2000 K.

4.1 Melting of Bulk Copper with Spherical Voids

Figure 4.1 shows the plots between various thermodynamic properties and temperature for all the systems.
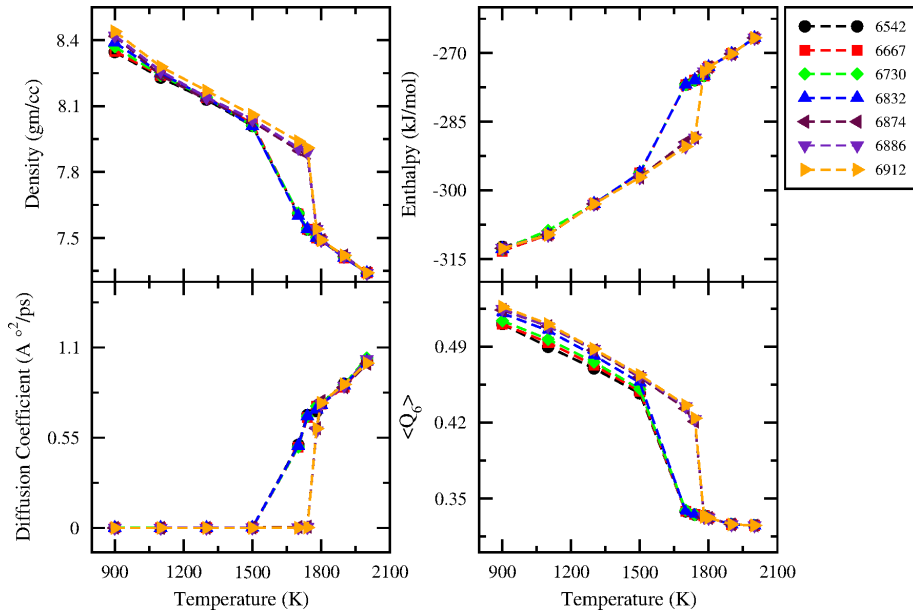

Figure 4.1: Density, enthalpy, diffusion coefficient and average bond order parameter as a function of temperature of bulk copper with different sized-voids and without voids.

For all systems and for all properties a sharp transition is observed. Systems with spherical voids greater than 5 Å melts earlier than other systems. Spherical voids of 4 and 5 Å melts at similar temperature to bulk. Atomic density and bond

31

order parameter (Q_6) decrease linearly with temperature till 1500 K then it drops sharply. Diffusion coefficient and enthalpy gradually increases with temperature and then at melting increases sharply. Four systems start melting at 1500 K and the other three melts at 1740 K. When we increase the temperature, the interatomic distance between two atoms decreases so that atomic density decreases and potential energy increases hence enthalpy of the system increases.

Diffusion coefficient gives the atomic motion before and after the melting point and is calculated from the slope of the mean square displacement (MSD) which is a measure of the average distance that a particle or an atom in a system travels. For large void systems (6-10 Å), the value of diffusion coefficient is low at 900-1500 K because the atoms are still in their original lattice position and the atomic motion is very low, but at 1780 K when the atoms are displaced from their lattice positions, the diffusion coeffficient reaches a maximum value of 0.55 Å$^2/ps$, which shows that atoms are now free to move. It is observed that for small void systems(4 and 5 Å) and void free Cu crystal, melting happens at around 1700 K.

The value of bond order parameter (Q_6) decreases with increasing temperature for all systems which shows that with increasing temperature the crystallinity of the solid decreases. At 1500 K, the atoms of the large void systems (6-10 Å) start to melt and by 1700 K they melt completely. The sudden drop of Q_6 value indicates that the atoms are displaced from their lattice positions. The value of Q_6 drops to a minimum of 0.332 at 1780 K and the crystal structure become disordered which means by 1780 K the crystal has melted completely.
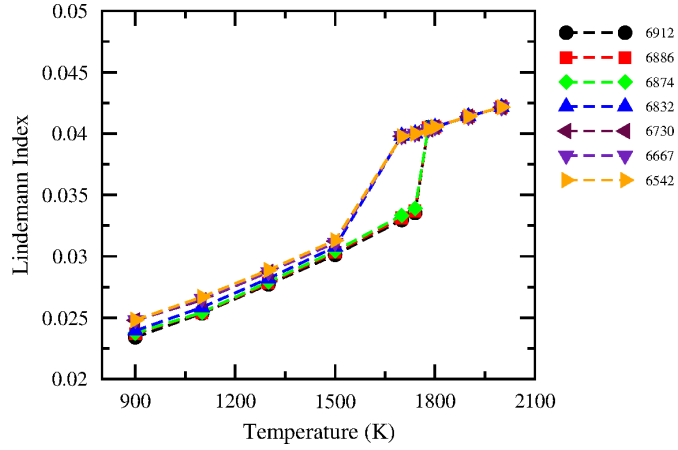
Figure 4.2: Lindemann index for the different size of voids system during heating process.

Figure 4.2 shows the behavior of lindemann index as a function of temperature. From the figure, it is found that the melting point of copper crystal of large spherical voids is 1500 K and for small void systems, it is around 1740 K which is identical to copper crystal without void.

For crystal systems containing voids of radius greater than 6 Å, when the temperature is lower than 1500 K, the lindemann index increases linearly with temperature. At 1500 K, the crystals melt and by 1700 K the value of lindemann index reaches a maximum of about 0.040 which means the atoms are completely displaced. Before 1500 K, the value of lindemann index is very low since most of the atoms donot have large vibrational amplitude motion, they vibrate around their original lattice positions which means the atoms of the large void systems are still in solid. After 1500 K, the atoms have large vibrational amplitude and start to melt, therefore, the value of lindemann index goes maximum.

But for small voids of radius 4, 5 Å and void free copper crystal, the lindermann index reaches a maximum value of 0.0405 at 1780 K indicating that crystal melts by 1780 K.
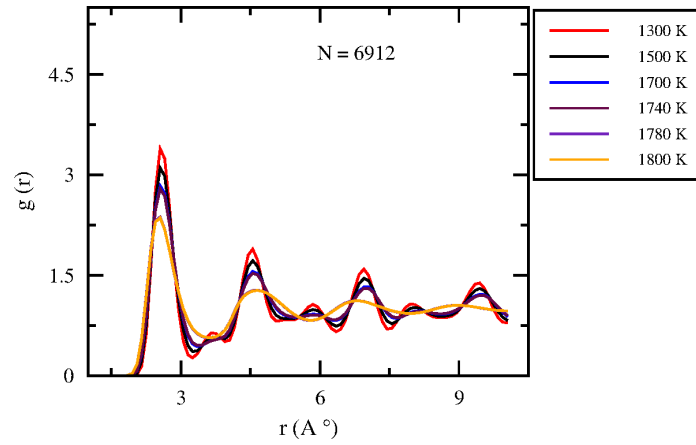
33

Figure 4.3: Radial distribution function of bulk copper at various temperatures.

Figure 4.3 shows the behavior of RDF for bulk copper system. The intensity of third and fourth peak is very low at 1780 K. This further illustrates the loss of long range order in the crystal when melting happens. At 1780 K, atoms in the bulk system behave like liquid. Loss of long range order along with change in the coordination of the first shell indicates the appearance of the molten state.
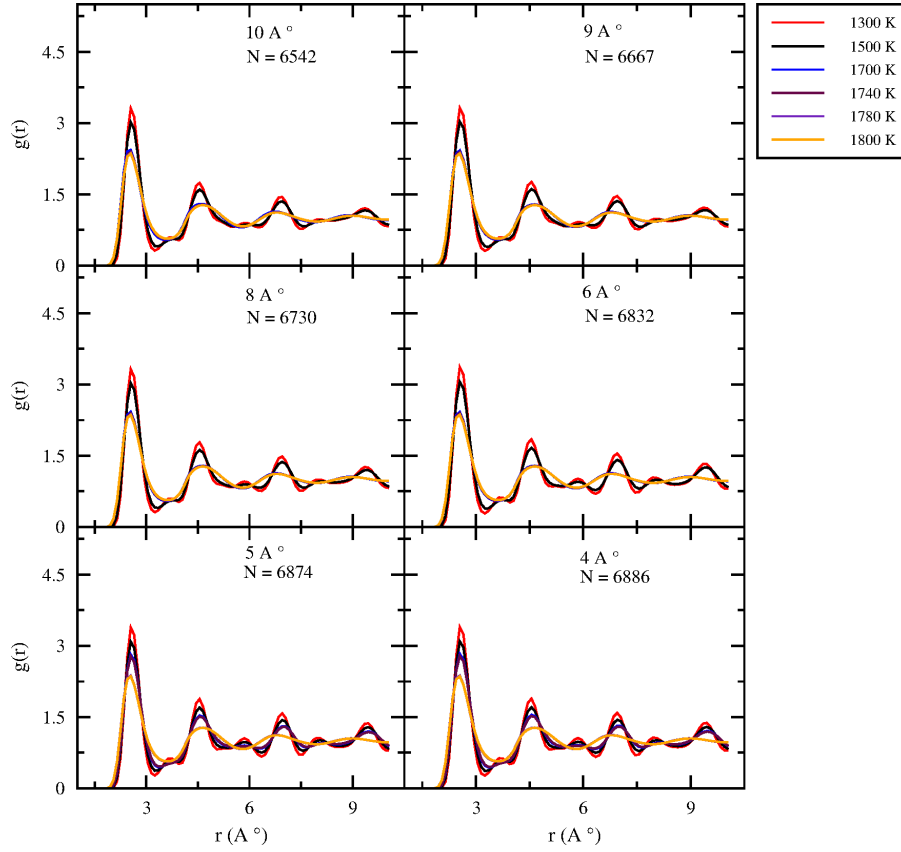
Figure 4.4: Radial distribution function of of voids system at various temperatures.

Figure 4.4 shows the behavior of radial distribution function for different size of voids system as a function of temperature. From the figure, it is observed that there are many sharp peaks which indicate that the atoms occupy fixed positions in first, second and subsequent shells. The peaks of the RDF for 6-10 Å void size, crystal systems are mostly sharp before 1700 K indicating the atoms are placed around each other. The peaks widen at higher temperature (after 1500 K) due to the thermal motion. At 1500 K the third and fourth peak disappears with appearance of molten state. But for 4 and 5 Å void size copper crystal and for void free copper crystal, the RDF peaks are intense till 1740 K. The third and fourth peaks disappear at 1780 K indicating the atoms of these systems are solid at 1740 K and liquid at 1780 K.

We calculated the fraction of cordination number from 9-16 for copper atoms using the following equation -

$$\langle f_{9,10,11,12,13,14,15,16} \rangle = \frac{n_{9,10,11,12,13,14,15,16}}{N} \qquad (4.1)$$

Where N = (total number of atoms) × (total number of configurations)

We have found that fraction of coordination with 12, 13 and 14 is more than 87%. We all know that in the solid state, the coordination number for fcc copper is 12.
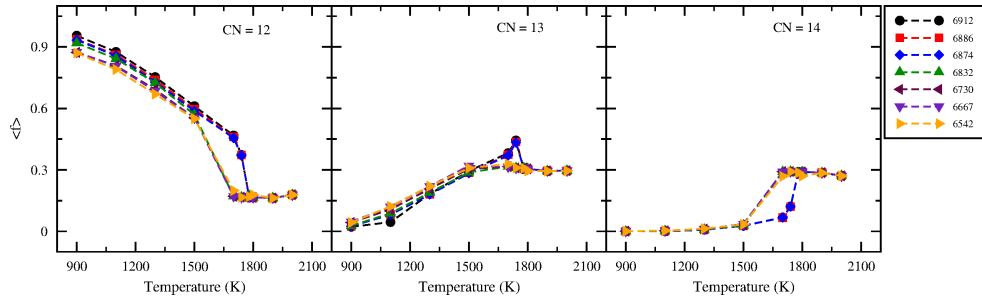

Figure 4.5: Fraction of copper atoms with 12, 13 and 14 neighbours of different systems as a function of temperature.

Figure 4.5 shows the variation of 12, 13 and 14 coordinated copper with temperature. Sharp changes in coordination concentration is observed for all these systems. It is also observed that for the system having void radius greater than 5 Å, 12 co-ordinated copper remains constant till 1500 K thereafter it sharply decreases. This drop in 12 coordinated copper is almost 40%. On the other hand concentration of 13 and 14 coordinated copper increases at melting. But for bulk and other two systems having void radius 4 and 5 Å, it is observed that most of the copper atoms are 12 coordinated till 1740 K and drops to a minimum value of 0.165 at 1780 K.

Figure 4.6: Distribution of orientational order parameter, Q_6 for coordination number 12, 13 and 14 at different temperatures of bulk copper.

Figure 4.6 shows the orientational ordering in 12, 13 and 14 coordinated atoms of bulk copper system at different temperatures. It is observed that two sharp peaks appear for all the coordinations and 12 coordinated copper atoms are more orientationally ordered following 13 and 14 coordinated atoms. The peak at higher q6 corresponds to crystalline state while the peak at higher q6 corresponds to the liquid state. Bond orientational order bulk molten state appears at 1780 K.
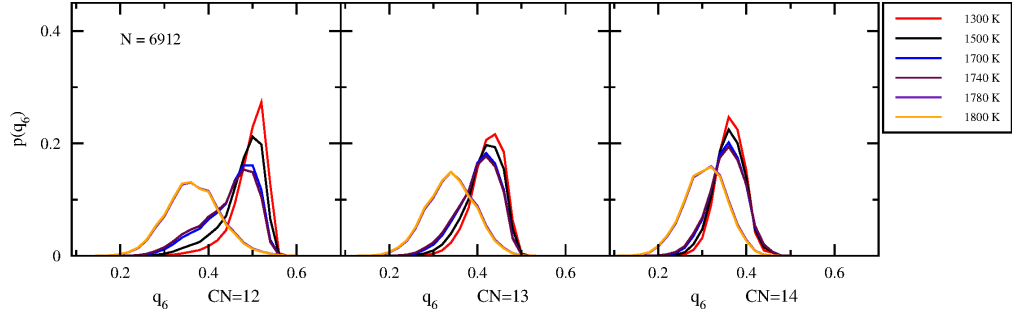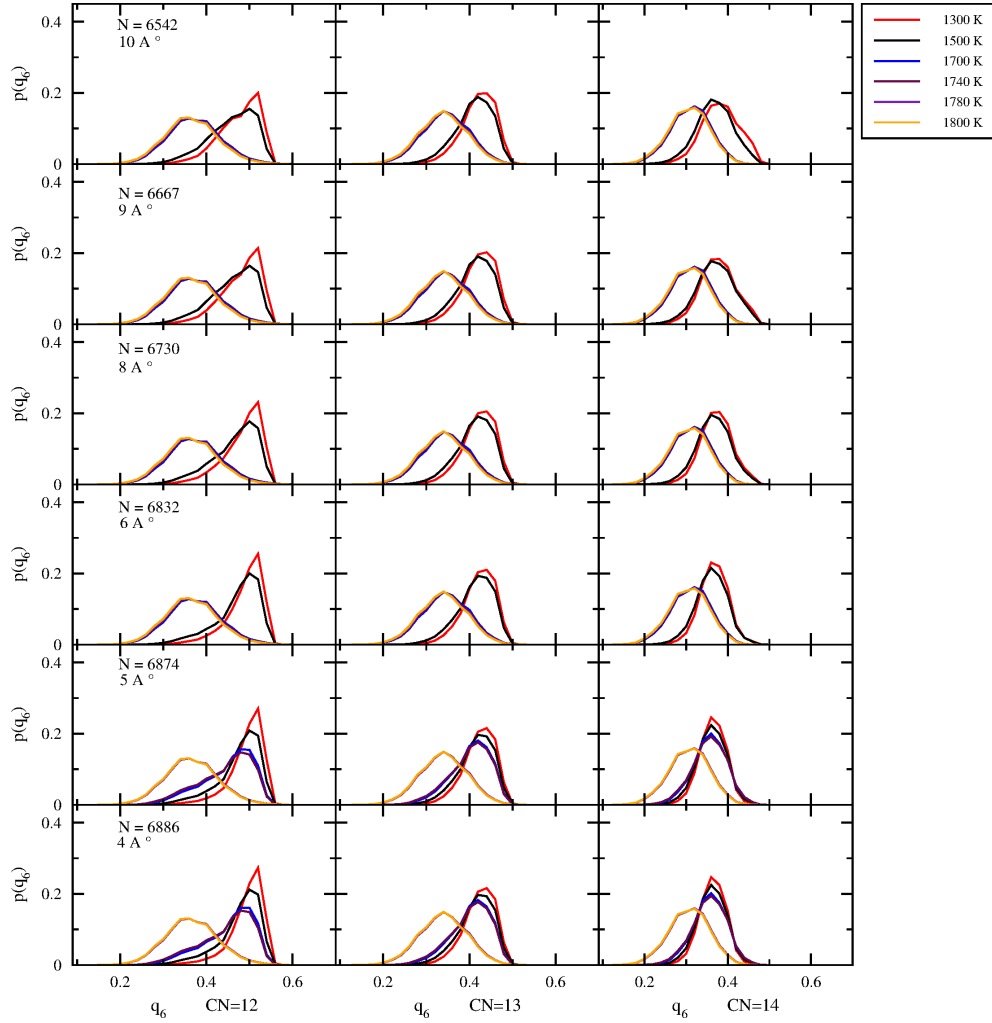
Figure 4.7: Distribution of orientational order parameter, Q_6 for coordination number 12, 13 and 14 at different temperatures.

Figure 4.7 shows the orientational ordering in 12, 13 and 14 coordinated copper atoms of all spherical void systems at different temperatures. We note here that for all the coordinations two sharp peaks appear. The peak at higher q6 corresponds to crystalline arrangemet and the peak at lower q6 corresponds to the liquid-like arrangement. It is also observed that 12 coordinated atoms are the most ordered and 14 coordinated atoms are the least. It may be noted that we chose to understand the crystallinity in these systems because 12, 13 and 14 coordinated copper all together consitute 90 % of the atoms in the crystal. Similar to previous results which show voids greater than 5 Å melts earlier than 4 Å, 5 Å and bulk systems. But we interestingly note that for 4 Å, 5 Å and bulk system melting in

12, 13 and 14 coordinated atoms take place at 1780 K, but for 6 Å and higher radii spherical voids melt at 1700 K. It must be remembered that we noted the melting temperatures at 1700 K for crystal systems having void radius 4 and 5 Å but here from bond-orientational order parameter bulk molten state appears at 1780 K. It signifies the existence of cryistallinity in differently coordinated system to a somewhat higher temperature.

4.2   Melting of Bulk Copper with Layered Voids

From our previous simulation results we conclude that melting in 6 Å and higher spherical voids happens earlier than 4 and 5 Å voids. Here we create a different shaped void by removing same number of atoms which are missing in the 10 Å void. Moreover we also remove these many atoms from two different positions of the crystals. We remove them from the (i) center and (ii) edge of the bulk copper system having 6912 atoms and performed molecular dynamics simulation at 1 bar and different temperatures varied from 900 to 2000 K. We analyze the properties like density enthalpy, diffusivity and radial distribution function and compare these properties with large void system of void radius 10 Å , which also contains 6542 atoms.
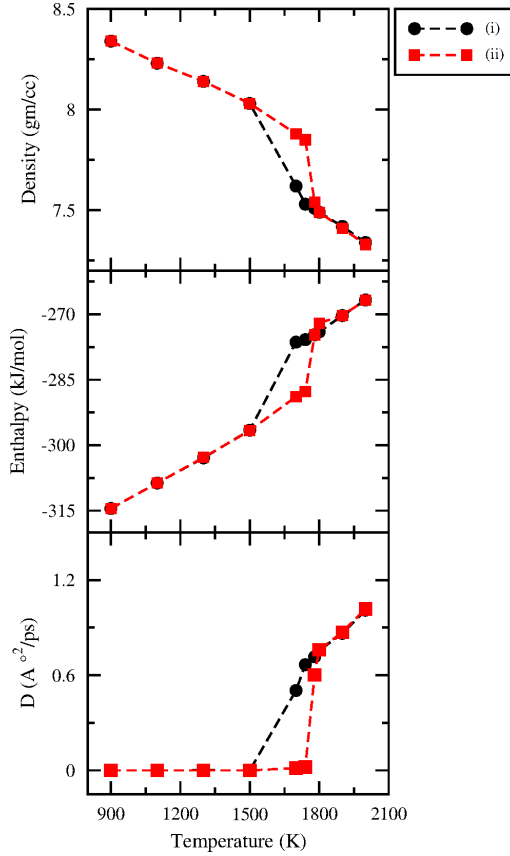
Figure 4.8: Density, enthalpy and diffusion coefficient as a function of temperature of bulk copper with layer voids.

From the figure 4.8, it seen that density, enthalpy and difusivity follow the same pattern with other crystal systems which we have already discussed in our previous section of this chapter.

The properties obtained from the system (i) behave exactly same as the system having void radius 10 Å. The atoms of the system (i) start to melt at 1500 K and are completely melted at 1700 K. But in the case of system (ii), it seems different. Though system (ii) also contains 6542 atoms, the phase transformation occurs at 1740 where solids turn to liquids. At this point density suddenly drops to a minimum value and enthalpy as well as the value of diffusion coefficient reach a maximum value following the same pattern with bulk copper and smaller void crystal systems having 4 and 5 Å void radii. We can conclude that melting temperature depends on the number of atoms removed to create the void but not

on the shape of the void. But melting temperature does depend on the position of the void created. Here layered voids created at the edges behave like melting of bulk copper.
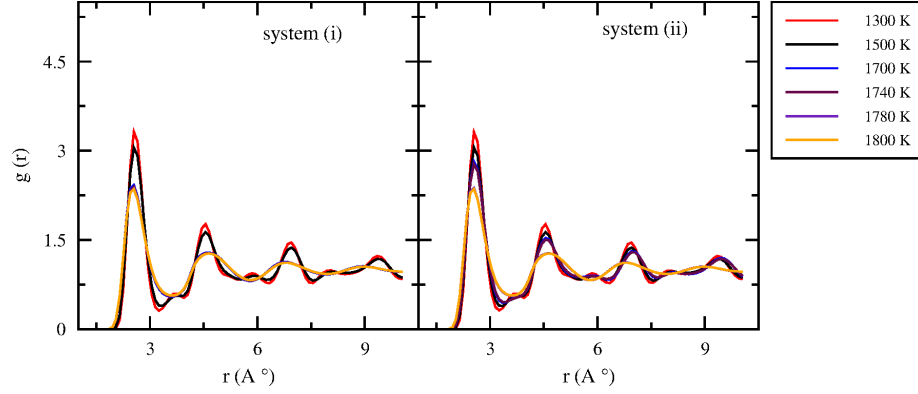
Figure 4.9: RDF of copper with layer voids at various temperatures.

Figure 4.9 shows the behavior of radial distribution function of sysytem (i) and system (ii) at various temperatures. RDF of system (i) also follows the same pattern with other crystal systems having void radius greater than 5 Å. The peaks are broad after 1500 K and the third and fourth peak have disappeared with increasing temperature indicating liquid like behavior of copper atoms. While the behavior of RDF for system (ii) is identical to the smaller void systems of radius 4 and 5 Å.

5 Conclusion and Future Prospects

5.1 Conclusion

The main objective of our reasearch work was to locate and understand melting of copper metal with volume voids. Before introducing the defects, we simulated a small crystal system of copper containing 500 atoms using molecular dynamics simulation at 1 bar. Two interatomic potentials, EAM and COMB were used for the simulation of 500 copper atoms. We found that densities obtained from both the poteintial were different. The melting point was found to be 1780 K by EAM potential which is closer to the available theoretical data [22]. Also EAM calculations were five times faster than COMB calculations. For that reason we decided to use only EAM potential for rest of our simulations.

After confirmation of melting point for the pure fcc copper, we introduced spherical voids into the pure copper crystal system containg 6912 atoms.The radius of spherical voids varied from 4-10 Å. We simulated these systems at 1 bar and temperatures were varied from 900 to 2000 K. The properties like density, entalpy, diffusivity and bond order parameter vary linearly after and before the transition. At transition all these properties show a sharp change. Lindemann index also varies linearly with temperature and at certain point it also increases sharply indicating the phase transition. Analyzing these properties obtained from the simulation we conclude that melting temperature decreases as the size of the volume voids increases. Crystal systems having void radius greater than 5 Å started to melt early temperature (1500 K) than the atoms of the 4 Å and 5 Å void size system which started to melt at 1700 K.

We also analyzed the behavior of radial distribution function and distribution of orientational order parameter, Q_6 for coordination number 12, 13 and 14 at different temperatures. We found that the second shell peak in the RDF and orientational order in 12 of the 6, 8, 9 and 10 Å spherical voids disappeared at 1700 K. But for bulk copper and for void size of 4 and 5 Å, orientational order in

12 disappeared at 1780 K indicating liquid like behavior of copper atoms.

The influence of other kinds of defect like layer defect is also studied. We removed 370 atoms from the center (i) and edge (ii) of bulk copper system containing 6912 atoms. We analyzed the structural and dynamics properties at 1 bar. We created these defects by removing the same number of atoms which were missing in the 10 Å void. It was found that system (i) behaved exactly same as the system having void size of 10 Å but system (ii) melted like bulk copper. Our results also confirm earlier observations that voids or defects created with removal of similar number of atoms melt at the same temperature [29]. But we also observe that position of the void effects melting. Removal of atoms from the edge has no effect on the melting transition. It resembles melting in bulk.

From our results we also underline key aspects of melting which are similar in bulk copper and in copper with volume voids - melting happens with loss of long-range order. 12 coordinated fraction decreases with appearance of molten state and the crystallinity within also disappears with melting. Interestingly loss of longe range order, loss of 12 coordinated copper happens at similar temperature but crystallinity is lost at somewhat higher temperatures (40 K higher). Volume voids created with removal of similar number of atoms melts at similar temperatures and melting is similar to bulk. Volume voids created at the edge of a crystal has negligible effect on bulk melting. Volume defects with sizes greater than 6 Å decreases melting temperature substantially.

5.2 Future Prospects

Few aspects of melting which needs to be investigated further are discussed here in this section. We need to investigate the reason behind appearance of plateau in melting temperature with increase in size of spherical voids. This has ben reported earlier and we also observe this from our study- spherical voids of 6, 8 and 10 Å behave similarly. We also need to understand why there is change in melting

temperature when the position of the void changes. Defects/voids weaken the system and facilitate thermal motion of atoms as well as propagation of defects. But defects within the crystal facilitates melting than defects at the surface. We also need to understand the behaviour of atoms which are at the interface of the void. Their behaviour is crucial to understand the melting transition. Finally one of the most important aspect of study of melting lies in understanding the kinetics of it. How fast voids appear/disappear, propagate etc.? These in-depth analysis will provide us with additional insights in understanding melting.

6 References

[1] Slava Sorkin. *Point Defects, Lattice Structure and Melting*. Technion-Israel Institute of Technology, Faculty of Physics, 2003.

[2] V Sorkin, E Polturak, and Joan Adler. Molecular dynamics study of melting of the bcc metal vanadium. i. mechanical melting. *Physical Review B*, 68(17):174102, 2003.

[3] FR Lindemann. Lindemann, fr, 1910, z. phys. 11, 609. *Z. Phys.*, 11:609, 1910.

[4] FD Stacey and RD Irvine. Theory of melting: thermodynamic basis of lindemann's law. *Australian Journal of Physics*, 30(6):631–640, 1977.

[5] Lewis H Cohen, William Klement Jr, and George C Kennedy. Melting of copper, silver, and gold at high pressures. *Physical Review*, 145(2):519, 1966.

[6] Max Born. Thermodynamics of crystals and melting. *The Journal of Chemical Physics*, 7(8):591–603, 1939.

[7] Amit Kanigel, Joan Adler, and Emil Polturak. Influence of point defects on the shear elastic coefficients and on the melting temperature of copper. *International Journal of Modern Physics C*, 12(05):727–737, 2001.

[8] BB Karki, GJ Ackland, and J Crain. Elastic instabilities in crystals from ab initio stress-strain relations. *Journal of Physics: Condensed Matter*, 9(41):8579, 1997.

[9] Jinghan Wang, Ju Li, Sidney Yip, Simon Phillpot, and Dieter Wolf. Mechanical instabilities of homogeneous crystals. *Physical Review B*, 52(17):12627, 1995.

[10] Yakovich Ilich Frenkel. Kinetic theory of liquids. 1955.

[11] JE Lennard-Jones and AF Devonshire. Critical and co-operative phenomena. iii. a theory of melting and the structure of liquids. *Proceedings of the Royal*

Society of London. Series A, Mathematical and Physical Sciences, pages 317–338, 1939.

[12] JE Lennard-Jones and AF Devonshire. Critical and co-operative phenomena. iv. a theory of disorder in solids and liquids and the process of melting. *Proceedings of the Royal Society of London. Series A, mathematical and physical sciences*, pages 464–484, 1939.

[13] Puneesh Puri and Vigor Yang. Effect of voids and pressure on melting of nano-particulate and bulk aluminum. *Journal of Nanoparticle Research*, 11(5):1117–1127, 2009.

[14] Amit Samanta, Mark E Tuckerman, Tang-Qing Yu, and E Weinan. Microscopic mechanisms of equilibrium melting of a solid. *Science*, 346(6210):729–732, 2014.

[15] JF Lutsko, D Wolf, SR Phillpot, and S Yip. Molecular-dynamics study of lattice-defect-nucleated melting in metals using an embedded-atom-method potential. *Physical Review B*, 40(5):2841, 1989.

[16] P Heino, H Häkkinen, and K Kaski. Molecular-dynamics study of copper with defects under strain. *Physical Review B*, 58(2):641, 1998.

[17] Karsten W Jacobsen, Per Stoltze, and JK Nørskov. A semi-empirical effective medium theory for metals and alloys. *Surface Science*, 366(2):394–402, 1996.

[18] Li-Bo Han, Qi An, Rong-Shan Fu, Lianqing Zheng, and Sheng-Nian Luo. Melting of defective cu with stacking faults. *The Journal of chemical physics*, 130(2):024508, 2009.

[19] SM Foiles, MI Baskes, and Murray S Daw. Embedded-atom-method functions for the fcc metals cu, ag, au, ni, pd, pt, and their alloys. *Physical review B*, 33(12):7983, 1986.

[20] William G Hoover. Canonical dynamics: equilibrium phase-space distributions. *Physical review A*, 31(3):1695, 1985.

[21] J Stadler, R Mikulla, and H-R Trebin. Imd: a software package for molecular dynamics studies on parallel computers. *International Journal of Modern Physics C*, 8(05):1131–1140, 1997.

[22] Li Wang, Yanning Zhang, Xiufang Bian, and Ying Chen. Melting of cu nanoclusters by molecular dynamics simulation. *Physics Letters A*, 310(2-3):197–202, 2003.

[23] HH Kart, H Yildirim, S Ozdemir Kart, and T Çağin. Physical properties of cu nanoparticles: A molecular dynamics study. *Materials Chemistry and Physics*, 147(1-2):204–212, 2014.

[24] AP Sutton and J Chen. Long-range finnis–sinclair potentials. *Philosophical Magazine Letters*, 61(3):139–146, 1990.

[25] Yue Qi, Tahir Çağin, and William A Goddard. Mpisim: Massively parallel simulation tool for metallic system. *Journal of computer-aided materials design*, 8(2-3):185–192, 2001.

[26] Jiacheng Zhang, Xinyun Wang, Yiying Zhu, Tielin Shi, Zirong Tang, Mo Li, and Guanglan Liao. Molecular dynamics simulation of the melting behavior of copper nanorod. *Computational Materials Science*, 143:248–254, 2018.

[27] Steve Plimpton. Fast parallel algorithms for short-range molecular dynamics. *Journal of computational physics*, 117(1):1–19, 1995.

[28] Jan Solca, Anthony J Dyson, Gerold Steinebrunner, Barbara Kirchner, and Hanspeter Huber. Melting curves for neon calculated from pure theory. *The Journal of chemical physics*, 108(10):4107–4111, 1998.

[29] Paras M Agrawal, Betsy M Rice, and Donald L Thompson. Molecular dynamics study of the effects of voids and pressure in defect-nucleated melting simulations. *The Journal of chemical physics*, 118(21):9680–9688, 2003.

[30] Xian-Ming Bai and Mo Li. Ring-diffusion mediated homogeneous melting in the superheating regime. *Physical Review B*, 77(13):134109, 2008.

[31] Jarosaw Meller et al. Molecular dynamics. *Encyclopedia of life sciences*, pages 1–8, 2001.

[32] Gemma Safont Camprubí. Mechanical properties at nano-level.

[33] Loup Verlet. Computer" experiments" on classical fluids. i. thermodynamical properties of lennard-jones molecules. *Physical review*, 159(1):98, 1967.

[34] Tao Liang, Bryce Devine, Simon R Phillpot, and Susan B Sinnott. Variable charge reactive potential for hydrocarbons to simulate organic-copper interactions. *The Journal of Physical Chemistry A*, 116(30):7976–7991, 2012.

[35] Murray S Daw and Michael I Baskes. Embedded-atom method: Derivation and application to impurities, surfaces, and other defects in metals. *Physical Review B*, 29(12):6443, 1984.

[36] Nadezhda Chistyakova and Thi My Hue Tran. A study of the applicability of different types of interatomic potentials to compute elastic properties of metals with molecular dynamics methods. In *AIP Conference Proceedings*, volume 1772, page 060019. AIP Publishing, 2016.

[37] Large-scale Atomic and Molecular Massively Parallel Simulator. Lammps users manual. 2003.

[38] Wei Cai. Handout 1. an overview of molecular simulation, 2005.

[39] Michael P Allen and Dominic J Tildesley. *Computer simulation of liquids*. Oxford university press, 2017.

[40] Anna Kucabal, Janusz Bytnar, and Zbigniew Walenta. Molecular dynamics computer simulation of nanoflows. In *Proceedings of the International Multiconference on ISSN*, volume 1896, page 7094, 2007.

[41] Gianluca Gregori. *Molecular dynamics simulations of the equilibrium dynamics of non-ideal plasmas*. PhD thesis, University of Oxford, 2012.

[42] Daan Frenkel and Berend Smit. *Understanding molecular simulation: from algorithms to applications*, volume 1. Elsevier, 2001.

[43] Shuichi Nosé. A unified formulation of the constant temperature molecular dynamics methods. *The Journal of chemical physics*, 81(1):511–519, 1984.

[44] Glenn J Martyna, Douglas J Tobias, and Michael L Klein. Constant pressure molecular dynamics algorithms. *The Journal of Chemical Physics*, 101(5):4177–4189, 1994.

[45] Hans C Andersen. Molecular dynamics simulations at constant pressure and/or temperature. *The Journal of chemical physics*, 72(4):2384–2393, 1980.

[46] William Humphrey, Andrew Dalke, and Klaus Schulten. Vmd: visual molecular dynamics. *Journal of molecular graphics*, 14(1):33–38, 1996.

[47] http://physics.nist.gov./PhysRefData/contents.html.

[48] Li Wei-Zhong, Chen Cong, and Yang Jian. Molecular dynamics simulation of self-diffusion coefficient and its relation with temperature using simple lennard-jones potential. *Heat TransferAsian Research: Co-sponsored by the Society of Chemical Engineers of Japan and the Heat Transfer Division of ASME*, 37(2):86–93, 2008.

[49] Feng Ding, Kim Bolton, and Arne Rosén. Molecular dynamics study of the surface melting of iron clusters. *The European Physical Journal D-Atomic, Molecular, Optical and Plasma Physics*, 34(1-3):275–277, 2005.

[50] Paul J Steinhardt, David R Nelson, and Marco Ronchetti. Bond-orientational order in liquids and glasses. *Physical Review B*, 28(2):784, 1983.

[51] Wolfgang Lechner and Christoph Dellago. Accurate determination of crystal structures based on averaged local bond order parameters. *The Journal of chemical physics*, 129(11):114707, 2008.

[52] https://lammps.sandia.gov/doc/compute_orientorder_atom.html.